

Role of transverse effective mass in Auger generation impacted planar III-V Tunnel FETs

Sheikh Z. Ahmed¹, Yaohua Tan², and Avik W. Ghosh^{1,3}

¹Charles L. Brown Department of Electrical and Computer Engineering, University of Virginia, Charlottesville, Virginia, USA. ²Synopsys, San Jose, California. ³Department of Physics, University of Virginia, Charlottesville, Virginia, USA. Email: sza9wz@virginia.edu

Introduction

The Tunnel field-effect-transistor (TFET) has widely been considered as one of the most viable replacements to the complementary metal oxide semiconductor (CMOS) devices due to their superior theoretical performance. Practically, though there have been scant demonstrations of the sub-60mV/dec of TFETs¹, it has yet to be realized at acceptable current levels over a substantial current swing needed for circuit operation. It is therefore imperative to study the primary delimiters of TFETs, mainly trap-assisted tunneling (TAT) and Auger generation²⁻⁴, along with ways to reduce them in order to improve device performance. The effect of TAT in TFETs has been studied extensively^{3,4}. Here, we study the role of transverse effective mass on Auger generation in a planar TFET and propose a method of improving device performance.

Results and Discussion:

Fig. 1. shows the double gated n-TFET simulated in this paper³. We consider a thin quasi-2D GaSb source and InAs channel/drain. Simulation studies demonstrated increased ON currents in ballistic TFETs by quantum confinement in the transverse direction. Quantum confinement leads to the creation of energy sub-bands in the device as shown in Fig. 2. The spacing ($E_2 - E_1$) between the sub-bands plays a crucial role in determining the tunneling probability. A low transverse effective mass increases this inter-spacing which effectively results in larger tunneling barrier width for the carriers and a low tunneling current. The Auger generation rate is a strong function of the conduction/valence bands density of states effective masses, m_c^* and m_v^* respectively. These masses have longitude and transverse components, m_l^* and m_t^* respectively with an overall effective mass $m^* = (m_t^{*2} m_l)^{1/3}$ ⁵. Here, we analyze the effect of varying the transverse component on the Auger generation rate.

Initially we vary m_t^* of the source and drain independently and the results are plotted in Fig. 3. Fig. 3(a) shows the relationship between the source/channel m_t^* and the device OFF current (at $V_{DS}=0.3V$ and $V_{GS}=0V$). The OFF current is dominated by the Auger generation current which is linked to the effective masses using the following relationship, $J_{aug} \propto \exp\left(-\frac{2\mu^{-1}+1}{\mu^{-1}+1} \frac{\Delta E}{kT}\right)$ where^{2,3} $\mu = m_c^*/m_v^*$. From this relationship we can deduce that increasing m_v^* leads to a reduced Auger current and rising m_c^* results in higher J_{aug} which is in agreement with the results in Fig. 3(a). The dependence of the ON current (at $V_{DS}=V_{GS}=0.3V$) on m_t^* is depicted in Fig. 3(b). As discussed earlier a heavier transverse mass reduces the tunneling barrier by lowering the sub-bands interspacing, which increases the tunneling ON current. In Fig. 3(c) we see the correlation between the ON/OFF ratio of the device current and m_t^* . We observe that increasing the source valence band (VB) mass can be used to improve device performance. On the other hand, increasing the channel conduction band (CB) mass does the opposite as it allows for a greater overlap of the VB and CB wavefunctions. In Fig. 4(a) we plot the transfer characteristics Auger current in comparison to the lowest reported InAs trap density yet, typical silicon trap density and ballistic current. We observe that if we reduce the trap density to levels in silicon, Auger current becomes a strong limiting factor for the subthreshold swing (SS). In Fig. 4(c) we add the ballistic current to the non-ideal currents. Fig. 4(c) shows the SS vs. drain current of the different currents of Fig. 4(b). Finally, we take a TFET where the source and channel has the same longitudinal masses. We then consider that they have same transverse mass and plot the $I_{DS}-V_{GS}$ characteristics in Fig. 5(a) for two different masses. Fig. 5(b) shows relationship between the ON/OFF ratio and different m_t^* .

Conclusion:

From our study we conclude that increasing transverse effective mass of the TFET materials by means of quantum confinement can enhance the device performance. In particular, the source valence band transverse effective mass can be a key factor in realizing the theoretical performances in practical TFETs.

References:

- [1] H. Lu et al., *IEEE Journal of the Electron Devices Society* 2.4 (2014): 44-49. [2] JT. Teherani et al., *JAP* 120.8 (2016): 084507. [3] SZ. Ahmed et al., *JAP* 124.15 (2018): 154503. [4] RN. Sajjad et al. *IEEE TED* 63.11 (2016): 4380-4387.
- [5] MA. Green, *JAP* 67.6 (1990): 2944-2954. [6] M Baik, Min, et al., *Applied Surface Science* 467 (2019): 1161-1169.

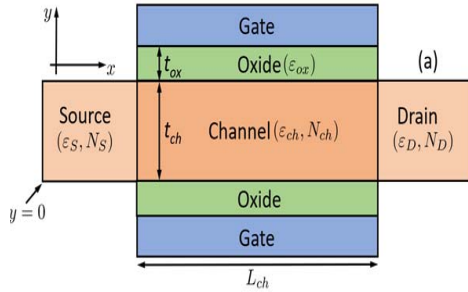


Figure 1. Simulated planar double gated heterojunction n-TFET³.

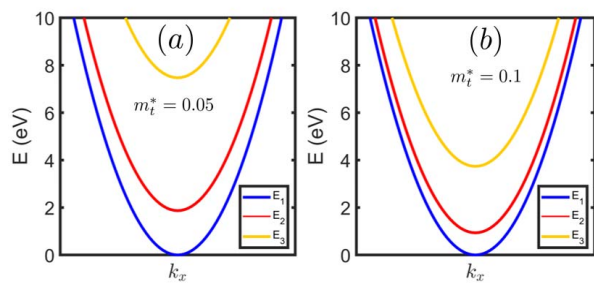


Figure 2. Quasi sub-bands in the transport direction using a simple $k.p$ model for (a) $m_t^* = 0.05$ (b) $m_t^* = 0.1$.

N_S	N_D	$m_{t,source}^*$	$m_{t,channel}^*$	t_{ch}	$E_{G,source}$	$E_{G,channel}$
$10^{19} cm^{-3}$	$5 \times 10^{17} cm^{-3}$	0.073	0.052	2nm	1.2eV	0.76eV

Table I. Major parameter values used in this simulation

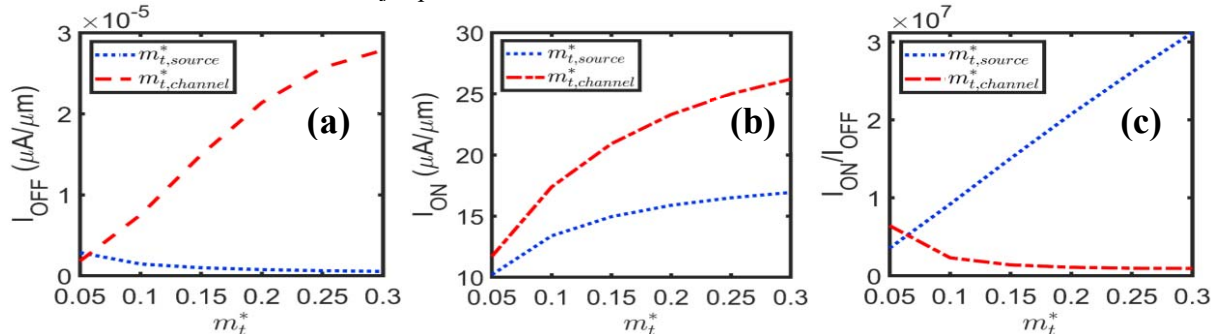


Figure 3. (a) OFF current dependence on $m_{t,source}^*$ and $m_{t,channel}^*$. (b) I_{ON} vs. transverse effective mass, m_t^* . Higher transverse mass, for both CB and VB, lowers interspacing between electronic sub-bands resulting in a smaller tunneling barrier width. (c) ON/OFF ratio vs. m_t^* . The ratio increases linearly with $m_{t,source}^*$ and decreases with $m_{t,channel}^*$.

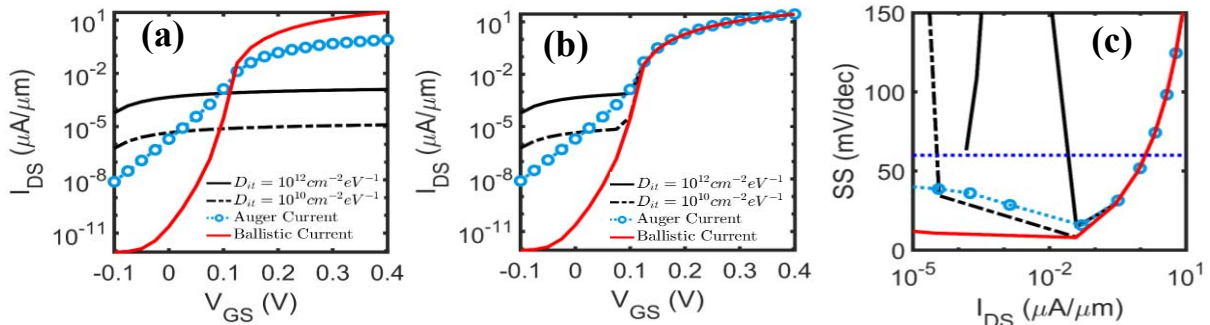


Figure 4.(a) I_{DS} - V_{GS} characteristics for lowest InAs trap density $D_{it} = 10^{12} cm^{-2} eV^{-1}$ reported⁶, for typical silicon density $D_{it} = 10^{10} cm^{-2} eV^{-1}$, Auger current and Ballistic current. (b) Ballistic current added to the non-ideal currents. (c) SS vs. I_{DS} for the different currents plotted in (b) in reference to the Boltzmann limit of 60mV/dec.

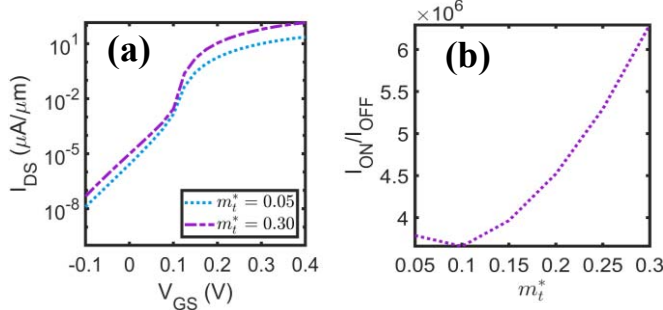


Figure 5. (a) I_{DS} - V_{GS} characteristics for an arbitrary TFET with previously mentioned longitudinal effective masses for the source and channel. We consider $m_t^* = 0.05$ and 0.3 for both the regions and compute the current. (b) The ON/OFF ratio for different m_t^* for this arbitrary TFET.